0026-895X/04/6605-1236–1247$20.00
MOLECULAR PHARMACOLOGY
Copyright © 2004 The American Society for Pharmacology and Experimental Therapeutics
Mol Pharmacol 66:1236–1247, 2004

Vol. 66, No. 5
893/1178282
Printed in U.S.A.

Molecular Determinants of Frequency Dependence and Ca^{2+} Potentiation of Verapamil Block in the Pore Region of $Ca_v1.2$

Nejmi Dilmac, Nathan Hilliard, and Gregory H. Hockerman

Department of Medicinal Chemistry and Molecular Pharmacology, School of Pharmacy and Pharmacal Sciences (N.H., G.H.H.) and Graduate Program in Biochemistry and Molecular Biology (N.D.), Purdue University, West Lafayette, Indiana

Received March 29, 2004; accepted July 28, 2004

ABSTRACT

Verapamil block of $Ca_v1.2$ is frequency-dependent and potentiated by Ca^{2+}. We examined the molecular determinants of these characteristics using mutations that effect Ca^{2+} interactions with $Ca_v1.2$. Mutant and wild-type $Ca_v1.2$ channels were transiently expressed in tsA 201 cells with β_{1b} and $\alpha_2\delta$ subunits. The four conserved glutamates that compose the Ca^{2+} selectivity filter in $Ca_v1.2$ were mutated to Gln (E363Q, E709Q, E1118Q, E1419Q) and the adjacent conserved threonine in each domain was mutated to Ala (T361A, T707A, T1116A, T1417A). The L-type-specific residues in the domain III pore region (F1117G) and the C-terminal tail (I1627A) were also mutated and assayed for block by verapamil using whole-cell voltage-clamp recordings in 10 mM Ba^{2+} or 10 mM Ca^{2+}. In Ba^{2+}, none of the pore-region mutations reduced the fraction of current blocked by 30 μM verapamil at 0.05 Hz stimulation. However, all of the pore-region mutations abolished Ca^{2+} potentiation of verapamil block at 0.05 Hz. The T1116A, F1117G, E1118Q, and E1419Q mutations all significantly reduced frequency-dependent verapamil block (1-Hz stimulation) in both Ba^{2+} and Ca^{2+}. The I1627A mutation, which disrupts Ca^{2+}-dependent inactivation, increased the fraction of closed channels blocked by 30 μM verapamil in Ba^{2+} but did not affect frequency-dependent block in Ba^{2+} or Ca^{2+}. Our data suggest that the pore region of domain III may contribute to a high affinity verapamil binding site accessed during 1-Hz stimulation and that Ca^{2+} binding to multiple sites may be required for potentiation of verapamil block of closed channels.

Ca^{2+} influx via voltage-dependent L-type Ca^{2+} channels (α_{1C}, $Ca_v1.2$) in cardiac and vascular smooth muscle initiates contractions and contributes to timing of the cardiac action potential (Bers and Perez-Reyes, 1999). $Ca_v1.2$ is sensitive to block by three distinct chemical classes of small-molecule drugs: dihydropyridines (DHPs), phenylalkylamines (PAAs), and benzothiazepines (BZPs) (Hockerman et al., 1997b). These drugs possess vasodilatory activity and are used to treat hypertension and angina pectoris (Fleckenstein and Fleckenstein-Grun, 1980). The $Ca_v1.2$ channel is a heteromultimer composed of a pore-forming α_1 subunit and regulatory β and $\alpha_2\delta$ subunits (Jones, 1998). The α_1 subunit is composed of four homologous domains (I–IV), each of which includes six transmembrane segments (S1–S6) (Tanabe et al., 1987). Each domain also includes a pore-lining region between segments 5 and 6, containing a conserved motif that features a Glu residue (EI, EII, EIII, EIV) that contributes to the Ca^{2+} selectivity filter (Yang et al., 1993). The large, intracellular C-terminal tail also contains an IQ calmodulin binding motif that is critical for the acceleration of the inactivation rate in Ca^{2+} relative to Ba^{2+} (i.e., Ca^{2+}-dependent inactivation) (Peterson et al., 1999; Zuhlke et al., 1999).

The PAA verapamil blocks $Ca_v1.2$ at low micromolar concentrations in both primary cardiac myocytes (Lee and Tsien, 1983) and heterologous expression systems (Johnson et al., 1996). Quaternary amine derivatives of verapamil and methoxyverapamil block $Ca_v1.2$ channels in smooth muscle cells only when applied to the intracellular side of the membrane, whereas a quaternary amine derivative of desmethoxyverapmil blocks $Ca_v1.2$ from either side of the membrane (Berjukov et al., 1996). Block of closed channels by desmethoxyverapamil involves specific amino acid residues in transmembrane segments IIIS6 and IVS6 that are unique to L-type channels (Hockerman et al., 1995, 1997a; Doring et al., 1996). PAAs preferentially block $Ca_v1.2$ channels undergoing high-frequency depolarizations, a property called frequency-dependent block (Lee and Tsien, 1983), which is the result of a higher drug affinity for the inactivated state of the channel (Johnson et al., 1996; Nawrath and Wegener, 1997).

This work was supported by Scientist Development Grant 9930016N from the American Heart Association (to G.H.H.).
Article, publication date, and citation information can be found at http://molpharm.aspetjournals.org.
doi:10.1124/mol.104.000893.

ABBREVIATIONS: DHP, dihydropyridine; PAA, phenylalkylamine; BZP, benzothiazepine; WT, wild-type; GFP, green fluorescent protein; D888, desmethoxyverapamil; ANOVA, analysis of variance.

Verapamil is not highly selective for L-type channels, because $Ca_v1.2$, $Ca_v2.1$, and $Ca_v2.3$ channels show little difference in sensitivity to verapamil (Cai et al., 1997). Thus, the binding site for PAAs may be substantially conserved across voltage-gated Ca^{2+} channels. Indeed, mutation of two of the conserved Glu residues to Gln in the selectivity filter of $Ca_v1.2$ (EIIIQ or EIVQ) reduces the affinity of desmethoxyverapamil for closed channels in Ba^{2+} (Hockerman et al., 1997a). We assayed $Ca_v1.2$ channels in which the conserved Glu residues were mutated to Gln [E363Q (EIQ), E709Q (EIIQ), E1118Q (EIIIQ), E1419Q (EIVQ)], or the adjacent conserved Thr residues to Ala [T361A (TIA), T707A (TIIA), T1116A (TIIIA), T1417A (TIVA)] for closed-channel block and frequency-dependent block by verapamil in Ba^{2+}. We found that none of the mutants tested significantly reduced the sensitivity of closed channels to block by verapamil but that EIIIQ, EIVQ, and TIIIA displayed a significantly lower extent of frequency-dependent block than did WT $Ca_v1.2$.

The conserved Glu residues that compose the selectivity filter of $Ca_v1.2$ bind Ca^{2+} ions as they pass through the channel pore, thus largely excluding monovalent cations when Ca^{2+} ions are present (Yang et al., 1993). However, the Ba^{2+} conductance of $Ca_v1.2$ is higher than that for Ca^{2+} because Ca^{2+} binds more tightly to the pore Glu residues (Almers and McCleskey, 1984). Ca^{2+} binding by $Ca_v1.2$ also modulates drug binding. All three chemical classes of L-type Ca^{2+} channel blockers are more potent when Ca^{2+}, rather than Ba^{2+}, is used as the charge carrier (Lee and Tsien, 1983). The conserved Glu residues in domains III and IV, as well as an adjacent Phe residue in the pore region of domain III in $Ca_v1.1$, mediate the Ca^{2+} potentiation of DHP (Peterson and Catterall, 1995) and diltiazem affinity (Dilmac et al., 2003). Furthermore, the IQ domain mutant I1627A potentiates diltiazem block of closed channels in Ba^{2+}, and Ca^{2+}-dependent inactivation is not required for Ca^{2+} potentiation of diltiazem block (Dilmac et al., 2003). We report here that Ca^{2+} potentiation of verapamil block of closed $Ca_v1.2$ channels is disrupted by any of the EQ or TA mutations. Furthermore, frequency-dependent block of $Ca_v1.2$ by verapamil in either Ba^{2+} or Ca^{2+} is also reduced in mutants with single amino acid substitutions at three adjacent positions in domain III (TIIIA, F1117G, EIIIQ) and in EIVQ. The C-terminal tail mutant I1627A increased the sensitivity of closed $Ca_v1.2$ channels to block by verapamil in Ba^{2+} but did not affect frequency-dependent block in either Ba^{2+} or Ca^{2+}.

Materials and Methods

Construction of Wild-Type and Mutant Ca^{2+} Channels. The $Ca_v1.2$ (Snutch et al., 1991) and mutant channels were subcloned into pcDNA3 (Invitrogen, Carlsbad, CA). Mutations were introduced as described previously (Hockerman et al., 1997a) or using a modification of the QuikChange site-directed mutagenesis procedure (Stratagene, La Jolla, CA). The desired mutations were verified and the integrity of the clones was confirmed by cDNA sequencing and extensive restriction digest analysis.

Cell Culture. Human tsA 201 cells, a simian virus 40 T-antigen-expressing derivative of human embryonic kidney 293 cells, were maintained in Dulbecco's modified Eagle's medium/Nutrient Mixture F-12 (Invitrogen) enriched with 10% fetal bovine serum.

Expression of Ca^{2+} Channels. Human tsA 201 cells were cotransfected with WT and mutant $Ca_v1.2$ α_1 subunits, β_{1b} (Pragnell et al., 1991) and $\alpha_2\delta$ (Ellis et al., 1988), and enhanced green fluorescent protein (GFP) (BD Biosciences Clontech, Palo Alto, CA) such that the molar ratio of the plasmids was 1:1:1:0.8. Cells were transfected using LipofectAMINE 2000 per the manufacturer's protocol (Invitrogen); cells were replated at low density for electrophysiological recording 20 to 24 h after transfection. Experiments were conducted 20 to 48 h after replating.

Electrophysiology. Transfected cells were recognized by GFP fluorescence at 510 nm with excitation at 480 nm. Barium and calcium currents through Ca^{2+} channels were recorded using the whole-cell configuration of the patch-clamp technique. Patch electrodes were pulled from VWR micropipettes (VWR, West Chester, PA) and fire-polished to produce an inner tip diameter of 4 to 6 μm. Currents were recorded using an Axopatch 200B patch-clamp amplifier (Axon Instruments Inc., Union City, CA) and filtered at 1 or 2 kHz (six-pole Bessel filter, -3 dB). Voltage pulses were applied and data were acquired using pClamp8 software (Axon Instruments Inc.). Voltage-dependent leak currents were subtracted using an on-line P/-4 subtraction paradigm. Verapamil, dissolved in bath saline, was applied to cells using an RSC 160 fast perfusion system (Bio-Logic, Claix, France) with constant exchange of the bath solution. I_{Ba} current was measured in the bath saline containing Tris (150 mM), $MgCl_2$ (4 mM), and $BaCl_2$ (10 mM). I_{Ca} current was measured in the same bath solution, except that Ca^{2+} (10 mM) replaced Ba^{2+}. The intracellular saline buffer contained *N*-methyl-D-glucamine (130 mM), EGTA (10 mM), HEPES (60 mM), MgATP (2 mM), and $MgCl_2$ (1 mM). (±)-Verapamil (Sigma/RBI, Natick, MA) concentrations were made from 100 mM stock solution in 70% ethanol. The pH of both solutions was adjusted to 7.3 with methanesulfonic acid. All experiments were performed at room temperature (20–23°C).

Data Analysis. Data were analyzed using Clampfit (Axon Instruments, Inc.) and SigmaPlot and SigmaStat software (SPSS Inc., Chicago, IL).

Results

Frequency-Dependent Drug Block and Ca^{2+} Potentiation of Drug Block in $Ca_v1.2$ Channels. Previous studies (Lee and Tsien, 1983) demonstrated that BZPs and PAAs, but not DHPs, show frequency-dependent block properties. Frequency-dependent block of the DHP nicardipine, the BZP diltiazem, and the PAA verapamil was assessed in our experimental system (Fig. 1A). Verapamil and diltiazem show strong frequency-dependent block of $Ca_v1.2$ channels, whereas the charged DHP nicardipine does not. Frequency-dependent drug block was measured in the presence of approximately IC_{50} concentrations of the indicated drugs in 10 mM Ba^{2+}. Whole-cell currents through WT $Ca_v1.2$ channels were measured using 100-ms depolarizations to +10 mV from a holding potential of -60 mV in the absence or presence of the indicated drug concentrations at 0.05 Hz. In cells to which drug was applied, block was allowed to reach equilibrium for several minutes at 0.05-Hz stimulation. The stimulation frequency was then increased to 1 Hz for 20 pulses. This procedure was applied in all subsequent experiments measuring frequency-dependent drug block.

Block of DHPs, BZPs, and PAAs is also potentiated by Ca^{2+} (Lee and Tsien, 1983). That is, the same concentration of drug will block a larger fraction of $Ca_v1.2$ channels when Ca^{2+}, rather than Ba^{2+}, is used as the charge carrier. Figure 1B shows Ca^{2+} potentiation of 30 μM verapamil block of WT $Ca_v1.2$. To determine Ca^{2+} potentiation of drug block, closed-channel block was measured as described at 0.05 Hz in 10 mM Ba^{2+} or 10 mM Ca^{2+}. Verapamil (30 μM) blocked a

greater fraction of Ca^{2+} current in Ca^{2+} than in Ba^{2+} (62% versus 34%). Thus, these two properties of verapamil block, frequency dependence and Ca^{2+} potentiation, are reconstituted in our experimental system.

Structural Features and Sites of Mutation in $Ca_v1.2$. The mutations in the pore region and C-terminal tail of L-type $Ca_v1.2$ channels used in this study are indicated and highlighted in Fig. 2, A and B. We used single amino acid mutants at each of the four highly conserved glutamates that form the selectivity filter. Negatively charged Glu residues were replaced with neutral Gln residues, individually, at the positions E363Q, E709Q, E1118Q, and E1419Q (EIQ, EIIQ, EIIIQ, and EIVQ) in each domain. Note that the structure of verapamil includes a tertiary amino group that is predominantly charged at physiological pH and could potentially interact with the acidic Glu side chains (Fig. 2C). Replacing glutamates with glutamines could potentially disrupt electrostatic interactions between the pore glutamates and both verapamil and Ca^{2+} ions. It is proposed that the negatively charged Glu1118 and Glu1419 residues may interact with the positively charged PAA desmethoxyverapamil via electrostatic interactions (Hockerman et al., 1997a). We also mutated the four highly conserved threonine residues adjacent to the critical Glu residues. These hydrophilic residues are conserved across all high-voltage-activated Ca^{2+} channels and are invariably located two positions upstream of the conserved Glu residues in each domain. Therefore, we singly mutated amino acids Thr361, Thr707, Thr1116, and Thr1417 to Ala (TIA, TIIA, TIIIA, and TIVA). In addition, we studied a mutant in which the L-type-specific residue in domain III, Phe1117, was mutated to Gly (F1117G). We previously demonstrated that the F1117G mutant disrupts frequency dependence and Ca^{2+} potentiation of $Ca_v1.2$ by diltiazem (Dilmac et al., 2003). Finally we studied the IQ motif mutant, I1627A, in the C-terminal tail of $Ca_v1.2$, because we previously reported that this mutant increases the affinity of the channel for diltiazem. Of all of these mutants, only TIA did not express functional channels.

Closed-Channel Block of the Glu-to-Gln Mutants by Verapamil in Ba^{2+}. WT and mutant EIQ, EIIQ, EIIIQ, and EIVQ $Ca_v1.2$ channels were coexpressed along with the $\alpha_2\delta$, β_{1b}, and GFP in tsA 201 cells by transient transfection. Forty-eight hours after transfection, whole-cell Ba^{2+} currents were measured in cells expressing the GFP marker.

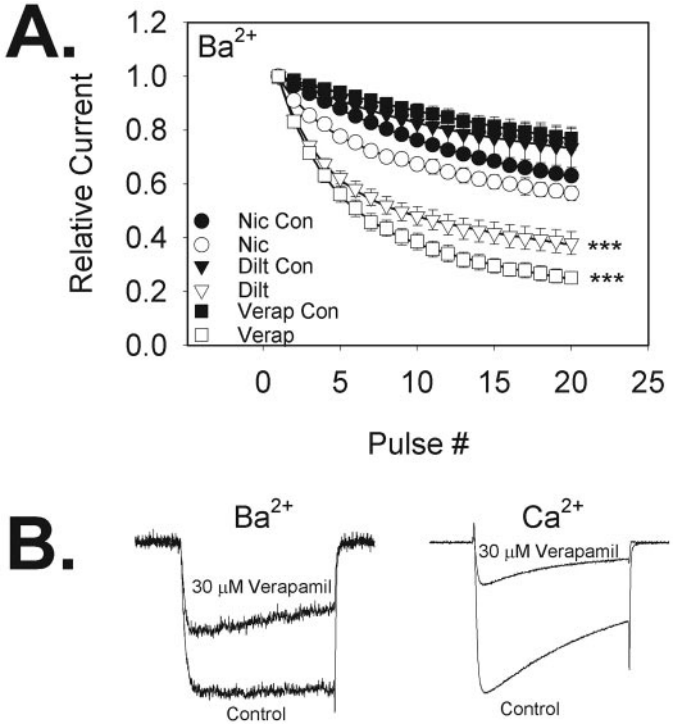

Fig. 1. Calcium potentiation of verapamil block and frequency dependence of block of WT $Ca_v1.2$ by structurally distinct drugs. A, frequency-dependent block of WT channels by approximately IC_{50} concentrations of the calcium channel blockers. Frequency-dependent block of WT channels was measured in the absence (closed symbols) or presence (open symbols) of 500 nM nicardipine, 50 μM diltiazem, and 30 μM verapamil. A frequency-dependent protocol was applied in which cells were depolarized from a holding potential of -60 mV to $+10$ mV for 100 ms every second. Note that, although nicardipine (charged DHP) did not show any frequency-dependent block accumulation, diltiazem (BZP) and verapamil (PAA) showed significant frequency-dependent drug block accumulation at the end of a 20-pulse stimulation. Block was brought to equilibrium with the indicated concentration of each drug at 0.05 Hz followed by a 20-pulse train of depolarizations given at 1 Hz. The asterisks indicate significant differences between the current remaining at the end of the train in the absence and presence of diltiazem or verapamil. B, verapamil block of WT channels at 0.05 Hz in Ba^{2+} or Ca^{2+}. Representative Ba^{2+} or Ca^{2+} currents recorded from tsA 201 cells expressing WT channels in the absence (control) or presence of 30 μM verapamil. Current was elicited using depolarizations to $+10$ mV from a holding potential of -60 mV for 100 ms every 20 s (0.05 Hz) (Student's t test; ★★★, $P < 0.001$) (mean ± S.E, $n = 3–8$).

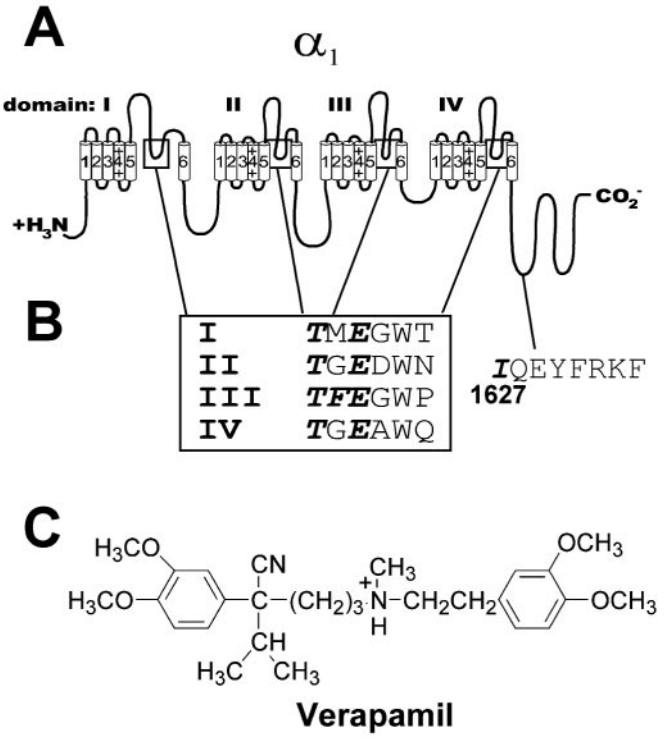

Fig. 2. Structural features of the α_1 subunit of $Ca_v1.2$. A, topology of $Ca_v1.2$ (α_{1C}). Cylinders represent transmembrane segments (1–6) organized into four homologous domains (I–IV). The C- and N-terminal domains are intracellular. Boxes highlight the putative pore-lining regions that contain the elements of the $Ca_v1.2$ selectivity filter. B, the amino acid sequences surrounding the Glu residues in each homologous domain that compose the selectivity filter. The conserved Glu and Thr residues are in bold italic type, as is the L-type-specific Phe residue directly adjacent to the conserved Glu residue in domain III (box). The approximate location of Ile 1627 and elements of the IQ Ca^{2+}/calmodulin binding domain are shown. C, chemical structure of verapamil. Note the ionizable tertiary alkylamino group.

Closed-channel block was measured from a holding potential of −60 mV using 100-ms depolarization to +10 mV at a frequency of 0.05 Hz. Increasing concentrations of verapamil (1, 5, 10, 50, or 100 μM) were applied to cells under voltage clamp. Representative traces recorded from WT in increasing verapamil concentrations in Ba^{2+} are shown in Fig. 3A. Drug block was brought to equilibrium for each dose, and current amplitude in the presence of drug was normalized to current amplitude in the absence of drug (Fig. 3B). Normalized current amplitudes at each verapamil concentration for several cells were averaged and plotted against drug concentration (Fig. 3B, inset). The verapamil IC_{50} value for WT was 40.5 ± 0.9 μM. The IC_{50} value for EIQ was not significantly different from that for WT channels (data not shown). Figure 3C shows the percentage of control current amplitude remaining for WT $Ca_v1.2$ and each of the EQ mutants in 30 μM verapamil at 0.05 Hz. The percentage of current remaining for all EQ mutants was not significantly different from that of WT $Ca_v1.2$. Thus, the mutation of any of the conserved glutamate residues does not change the sensitivity of the channel to closed-channel block by verapamil.

Frequency-Dependent Block of Glu-to-Gln Mutants in Ba^{2+}. Although none of the Glu-to-Gln mutants affected verapamil block of closed channels, we examined each mutant for frequency-dependent block by verapamil. Current was measured in the absence and presence of 30 μM verapamil in 10 mM Ba^{2+}. In the presence of drug, block was brought to equilibrium at 0.05 Hz followed by a train of 20 depolarizations at 1 Hz as described for Fig. 1. The peak amplitudes of the resulting current traces were normalized to the peak amplitude of pulse 1 of the 20-pulse train, and the averaged data were plotted against pulse number. Mutation of the conserved glutamate residues exhibited distinct effects on the frequency-dependent block of verapamil. Although EIQ and EIIQ did not significantly affect frequency-dependent block (Fig. 4A), accumulation of frequency-dependent block by verapamil was significantly reduced in EIIIQ and EIVQ (Fig. 4, B and C).

Ca^{2+} Potentiaion of Verapamil Block in WT and EQ mutants. We next assessed verapamil block of WT $Ca_v1.2$ and the Glu-to-Gln mutant channels using 10 mM Ca^{2+} as the charge carrier. First, we measured the percentage of control current remaining in the presence of 30 μM verapamil at 0.05 Hz (closed-channel block) and compared these values for each channel to those measured in 10 mM Ba^{2+} (Fig. 5A). Verapamil block of WT $Ca_v1.2$ was potentiated in Ca^{2+} relative to Ba^{2+} such that only 37.8 ± 1.5% of current remained in the presence of 30 μM verapamil in 10 mM Ca^{2+}, whereas 58.6 ± 2.6% of current remained in 10 mM Ba^{2+}. In contrast, the percentage of current remaining in the presence of 30 μM verapamil was not different in 10 mM Ba^{2+} or 10 mM Ca^{2+} in each of the Glu-to-Gln mutants. Thus, Ca^{2+} potentiation of verapamil block was eliminated in all of the Glu-to-Gln mutants, indicating that neutralization of any of the selectivity filter Glu residues uncouples Ca^{2+} binding from an increase in verapamil affinity.

We also examined frequency-dependent verapamil block in the $Ca_v1.2$ WT and Glu-to-Gln mutations using 10 mM Ca^{2+} as the charge carrier (Fig. 5, B and C). As we observed in Ba^{2+}, the EIQ and EIIQ mutants were not different from WT $Ca_v1.2$ in the extent of verapamil block accumulation by the end of a 1-Hz, 20-pulse train of depolarizations. However, the

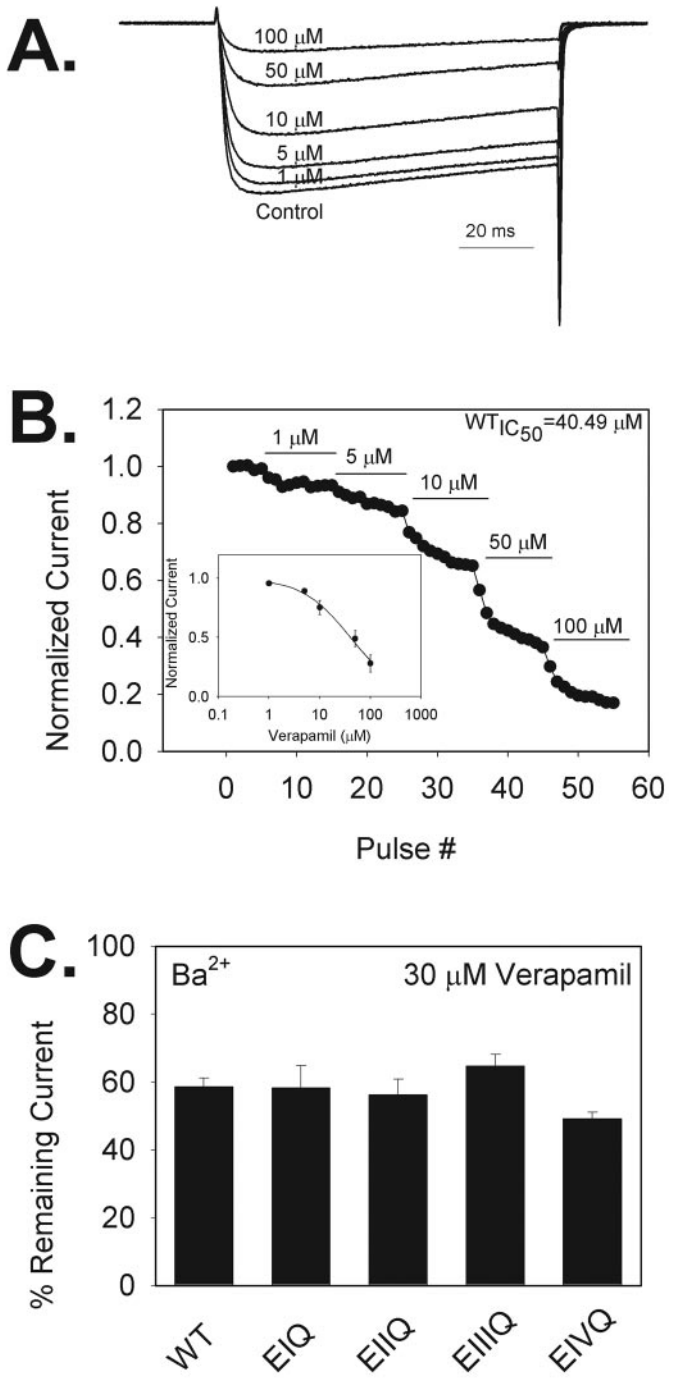

Fig. 3. Verapamil block of WT and the mutant channels EIQ, EIIQ, EIIIQ, and EIVQ at 0.05 Hz in Ba^{2+}. A, representative Ba^{2+} current recorded from a tsA 201 cell expressing transiently transfected WT channels in the absence (control) or presence of the indicated concentrations of verapamil. Pulses were from a holding potential of −60 mV to +10 mV for 100 ms every 20 s. B, dose-response relationships for WT channels. The averaged, normalized current amplitudes at 1, 5, 10, 50, and 100 μM verapamil were plotted against the corresponding drug concentration, and the IC_{50} value was determined by fitting the averaged relative current values at each verapamil concentration to the equation, relative current = 1 − {1/[1 − (IC_{50}/[verapamil])]} (inset). The IC_{50} value of the WT channels was 40.5 ± 0.9 μM. C, percentage of remaining currents of WT and the mutant channels in 30 μM verapamil. The remaining current values for each case (mean ± S.E. and n = 5–7) were: WT = 58.6 ± 2.6%; EIQ = 58.3 ± 6.5%; EIIQ = 56.3 ± 4.6%; EIIIQ = 64.7 ± 3.4%; EIVQ = 49.2 ± 1.9%. None of the mutant channels were significantly different from the WT channel in sensitivity to block by verapamil under these conditions (one-way ANOVA).

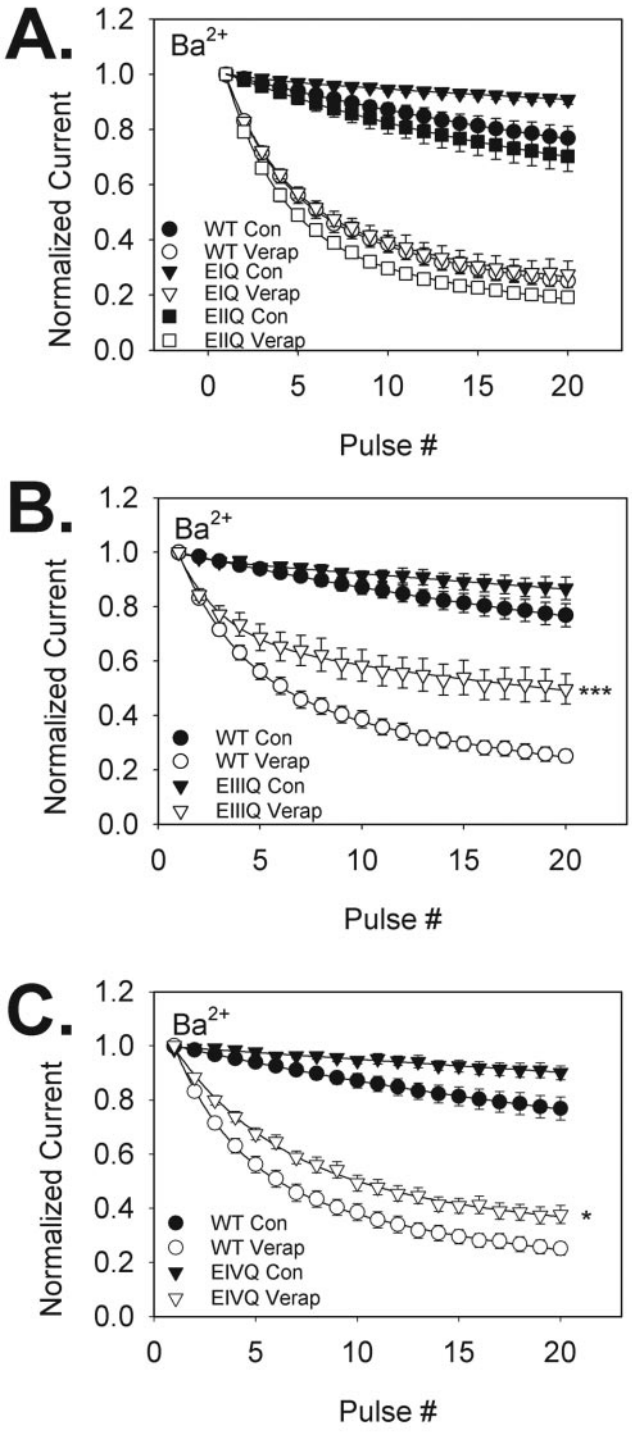

Fig. 4. Frequency-dependent verapamil block of WT and the mutant EIQ, EIIQ, EIIIQ, and EIVQ $Ca_v1.2$ channels. A to C, whole-cell Ba^{2+} currents were recorded in the absence and presence of 30 μM verapamil using depolarizations to +10 mV for 100 ms from a holding potential of −60 mV, at a frequency of 1 Hz for 20 pulses. Current measured in the presence of verapamil followed equilibration of block by 30 μM verapamil at 0.05 Hz. Relative peak current (mean ± S.E., n = 3–8) in each successive depolarizing pulse is plotted against pulse number in the absence (closed symbols) or presence (open symbols) of 30 μM verapamil for WT and the indicated mutant channels. Smooth lines are fits of the data to a single exponential equation, and these fits indicate that block reaches equilibrium at 25, 51, and 34% of control current for WT, EIIIQ, and EIVQ, respectively. The asterisks indicate that the fraction of current remaining at the end of the 20th pulse was statistically different from that of WT $Ca_v1.2$ channels (Student's t test; ⋆, $P < 0.05$; ⋆⋆⋆, $P < 0.001$).

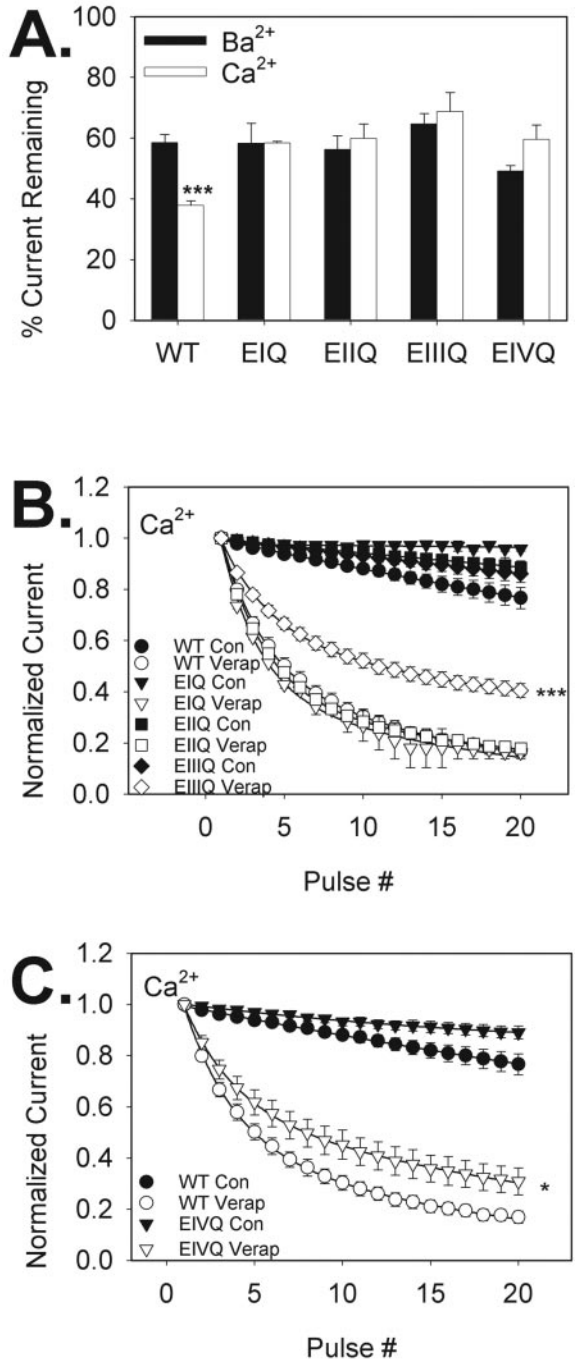

Fig. 5. Verapamil block of WT and Glu-to-Gln mutant $Ca_v1.2$ channels in Ca^{2+}. A, Ca^{2+} potentiation of verapamil block at 0.05 Hz. Verapamil (30 μM) was applied to tsA 201 cells expressing WT and the mutant channels under voltage clamp, as in Fig. 3C, using either 10 mM Ba^{2+} (closed bars) or 10 mM Ca^{2+} (open bars) as the charge carrier. The percentage of current remaining in each case was: WT_{Ba} = 58.6 ± 2.6; WT_{Ca} = 37.8 ± 1.5; EIQ_{Ba} = 58.3 ± 6.5; EIQ_{Ca} = 58.4 ± 0.6; $EIIQ_{Ba}$ = 56.3 ± 4.6; $EIIQ_{Ca}$ = 59.9 ± 4.7; $EIIIQ_{Ba}$ = 64.7 ± 3.4; $EIIIQ_{Ca}$ = 68.7 ± 6.4; $EIVQ_{Ba}$ = 49.2 ± 1.9; and $EIVQ_{Ca}$ = 59.6 ± 4.7. The asterisks indicate significant differences between current remaining in Ba^{2+} and Ca^{2+}. B and C, frequency-dependent block of the indicated channels in the absence (closed symbols) and presence (open symbols) of 30 μM verapamil was measured as described in Fig. 4 except that Ba^{2+} was replaced with 10 mM Ca^{2+}. Smooth lines are fits of the data to a single exponential equation, and these fits indicate that block reaches equilibrium at 17, 40, and 30% of control current for WT, EIIIQ, and EIVQ, respectively. EIIIQ and EIVQ channels were blocked to a significantly lesser extent than WT channels under these conditions (mean ± S.E, n = 3–8; Student's t test; ⋆, $P < 0.05$; ⋆⋆⋆, $P < 0.001$).

EIIIQ and EIVQ mutations both exhibited less accumulation of verapamil block under the same conditions. Surprisingly, we also observed that the extent of frequency-dependent verapamil block was not significantly different in the WT $Ca_v1.2$ channel whether we used 10 mM Ba^{2+} (23 ± 1.6% current remaining) or 10 mM Ca^{2+} (19 ± 2.0%; $P = 0.09$) as the charge carrier (see Figs. 4 and 5).

Kinetic Analysis of Depolarized Channel Block of WT and EIIIQ. To better understand the reduction in the frequency-dependent block of EIIIQ by verapamil, we compared the verapamil modulation of the voltage dependence and kinetics of inactivation in WT and EIIIQ. The voltage dependence of steady-state inactivation of WT and EIIIQ channels was measured in the absence and presence of 30 μM verapamil in Ba^{2+} (Fig. 6A). From a holding potential of −80 mV, cells were held at the indicated conditioning voltages for 10 s, followed immediately by a 100-ms test pulse to +10 mV. Normalized current amplitudes during the test pulses were plotted against the conditioning voltages. The data were fit to a Boltzman equation, and the voltage at which half the channels were inactivated during the conditioning pulse ($V_{1/2}$) was calculated. For WT and EIIIQ channels, $V_{1/2}$ was not significantly different in the absence of verapamil (−13.7 ± 0.5 mV versus −15.9 ± 0.6 mV, respectively). However, the leftward shift in $V_{1/2}$ induced by 30 μM verapamil was significantly greater in WT channels than in EIIIQ (−43.7 ± 0.8 mV versus −32.9 ± 0.4 mV, respectively) indicating that the EIIIQ mutant disrupted verapamil interaction with the inactivated state of the channel.

We also examined the time course of WT and EIIIQ channel recovery from depolarized channel verapamil block. Whole-cell Ba^{2+} current was equilibrated with 30 μM verapamil using 100-ms depolarizations to +10 mV from a holding potential of −60 mV at 0.05 Hz. After the current reached steady state, a 1-s depolarization to +10 mV was applied in the continued presence of drug, followed by a return to −60 mV. The recovery of the current after a 1-s depolarization to +10 mV in the presence or absence of drug was measured by depolarizing cells to +10 mV for 50 ms from −60 mV at intervals of 0.01, 0.1, 0.5, 1, 10, 20, and 30 s. To determine the fraction of WT and EIIIQ channels recovered from verapamil block, recovered current was expressed as a fraction of the peak current during the 1-s depolarization, plotted against recovery interval in the absence or presence of 30 μM verapamil, and fit to a double-exponential function (Fig. 6, B and C). The fast phase of recovery from inactivation (i.e., in the absence of drug) was similar in both WT and EIIIQ channels (WT: $\tau_{fast} = 283$ ms, $f_{fast} = 0.60$; EIIIQ: $\tau_{fast} = 213$ ms, $f_{fast} = 0.46$), whereas the slow phase of recovery was slower for EIIIQ (WT: $\tau_{slow} = 6.88$ s; EIIIQ: $\tau_{slow} = 16.9$ s). For the WT channel in the presence of 30 μM verapamil, both time constants for recovery were increased (WT: $\tau_{fast} = 1.83$ s, $\tau_{slow} = 41.0$; s $f_{fast} = 0.54$). For EIIIQ, 30 μM verapamil slowed the fast phase of recovery ($\tau_{fast} = 1.91$ s; $f_{fast} = 0.46$), but the time constant for the slow phase of recovery was actually accelerated in comparison to EIIIQ in the absence of drug ($\tau_{slow} = 8.07$ s). Thus, our results suggest that the marked decrease in frequency-dependent block of EIIIQ by verapamil compared with WT could be the result of faster dissociation of verapamil from EIIIQ at −60 mV. Recovery of current after a 1-s depolarization to +10 mV for EIIQ was not different from that for WT in either the absence or presence of 30 μM verapamil (data not shown).

Verapamil blocks $Ca_v1.2$ channels with higher affinity at depolarized potentials. As shown in Fig. 7, A and B, even after bringing current to steady state in the presence of 30 μM verapamil with depolarizations to +10 mV at 0.05 Hz, both WT and EIIIQ channels are rapidly and completely blocked during a 1-s depolarization to +10 mV. We compared the rate of current decay during a 1-s depolarization to +10 mV, from a holding potential of −60 mV, in the absence or presence of 30 μM verapamil for the WT and EIIIQ channels. Current traces were normalized to peak current and fit with a double-exponential function. In the absence of drug (Fig. 7B, filled bars), both WT and EIIIQ channels inactivated with virtually identical fast and slow time constants, and fractions of channels inactivating with each time constant (WT: $\tau_{fast} = 0.16 \pm 0.02$ s, $\tau_{slow} = 1.78 \pm 0.11$ s, $f_{fast} = 0.10 \pm 0.02$, $f_{slow} = 0.70 \pm 0.13$; EIIIQ: $\tau_{fast} = 0.15 \pm 0.06$ s, $\tau_{slow} = 1.46 \pm 0.53$ s, $f_{fast} = 0.12 \pm 0.04$, $f_{slow} = 0.62 \pm 0.07$). In the presence of 30 μM verapamil (Fig. 7B, open bars), WT and EIIIQ channel inactivation followed a single time constant and was virtually complete (WT: $\tau = 0.29 \pm 0.02$ s, $f = 1.02 \pm 0.02$; EIIIQ $\tau = 0.21 \pm 0.02$ s, $f = 1.05 \pm 0.01$ s). Thus, in both WT and EIIIQ channels, 30 μM verapamil blocks virtually all channels with a time course that resembles the fast-inactivating state, leading to complete inactivation by the end of a 1-s depolarization.

Effect of the F1117G and I1627A Mutants on Closed-Channel and Frequency-Dependent Block. Because both Phe1117 and Ile1627 have been implicated in modulation of $Ca_v1.2$ channel function by Ca^{2+} (Peterson and Catterall, 1995; Zuhlke et al., 1999), we examined their roles in both Ca^{2+} potentiation and frequency dependence of verapamil block. Block of closed F1117G and I1627A channels was measured at 0.05 Hz in 30 μM verapamil in Ba^{2+} or Ca^{2+} (Fig. 8A). Like the conserved pore glutamate mutants, the F1117G mutant disrupted Ca^{2+} potentiation of verapamil block such that current remaining in the presence of 30 μM verapamil was the same whether Ca^{2+} or Ba^{2+} was the charge carrier. Likewise, the extent of closed-channel verapamil block of the I1627A mutant was not different when measured in Ba^{2+} or Ca^{2+} from a holding potential of −60 mV. However, the percentage of I1627A current remaining in the presence of 30 μM verapamil in either Ba^{2+} or Ca^{2+} was not different from that of WT in Ca^{2+}. From a holding potential of −80 mV, the percentage of I1627A current remaining in 30 μM verapamil was not different from that of WT in either Ba^{2+} (70.1 ± 4.7) or Ca^{2+} (71.0 ± 2.4). Frequency-dependent block was measured in Ba^{2+} and Ca^{2+} in 30 μM verapamil at 1 Hz as described in Figs. 4 and 5. Although the I1627A mutant did not significantly affect accumulation of frequency-dependent block in either Ba^{2+} or Ca^{2+}, the F1117G mutant significantly reduced frequency-dependent block by verapamil at the end of a 20-pulse, 1-Hz train of depolarizations in either Ba^{2+} or Ca^{2+} (Fig. 8, B and C). Thus, whereas F1117G disrupts both Ca^{2+} potentiation and frequency dependence of verapamil block, I1627A enhances closed-channel verapamil block in Ba^{2+} to the level of that seen in Ca^{2+} with WT $Ca_v1.2$.

To better understand the basis for the observed differences in verapamil block of F1117G and I1627A, we measured the voltage dependence of inactivation for these two mutants in

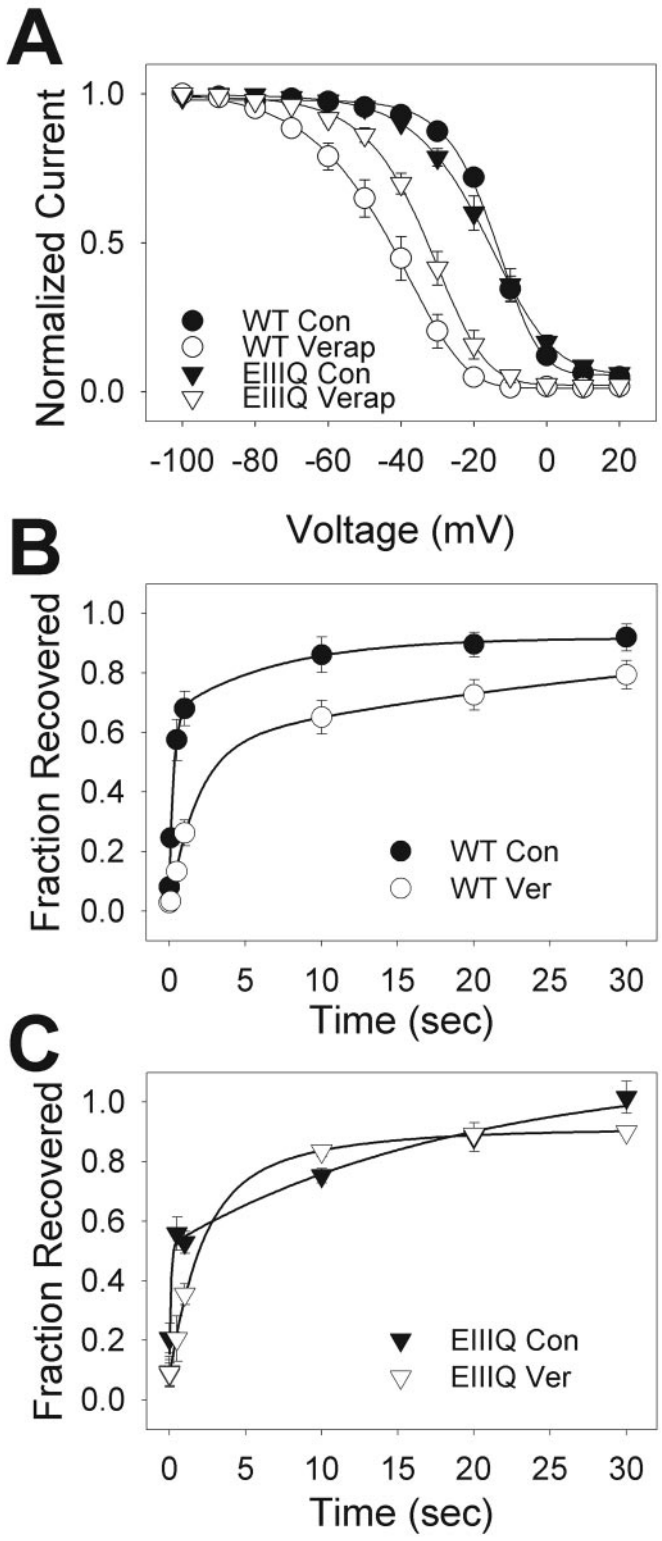

Fig. 6. Verapamil modulation of inactivation in WT and EIIIQ $Ca_v1.2$ channels. A, steady-state inactivation was measured by depolarization of tsA 201 cells to +10 mV for a 100-ms test pulse immediately after a 10-s conditioning pulse at the indicated potentials from a holding potential of −80 mV. Measured Ba^{2+} current was plotted against the conditioning pulse voltage in the absence (closed symbols) or presence (open symbols) of 30 μM verapamil. The data were fit to the equation, relative current = $1/\{1 - \exp[(V - V_{1/2})/k]\}$, where V is the conditioning potential, $V_{1/2}$ is the voltage at which half of the channels are inactivated, and k is a slope factor (potential required for an e-fold change). $V_{1/2}$ values for WT channels in the absence and presence of 30 μM verapamil were −13.7 ± 0.5 and −43.5 ± 0.8 mV, respectively. $V_{1/2}$ values for EIIIQ channels the absence and presence of 30 μM verapamil in 10 mM Ba^{2+} (Fig. 8D). Although the $V_{1/2}$ values in the absence of drug for both channels were shifted to more negative potentials compared with WT (F1117G, −23.4 ± 0.5 mV; I1627A, −28.4 ± 0.8 mV), the leftward shift in the presence of 30 μM verapamil was ~30 mV for both WT and I1627A channels but only ~12 mV for F1117G. Thus, despite the observation that both mutants cause a leftward shift in $V_{1/2}$, they are markedly different in the manner in which they interact with verapamil.

Frequency Dependence and Ca^{2+} Potentiation in the TA Mutants. Because mutation of two of the four selectivity filter Glu residues and the L-type-specific Phe1117 residue markedly reduced frequency dependence and Ca^{2+} potentiation of verapamil block, we examined the role of the adjacent, conserved Thr residues in each domain. We found that mutation of Thr361 in domain I to Ala is apparently not tolerated, because neither this single point mutant, nor a quadruple mutant, with the conserved Thr in each domain changed to Ala, yielded functional channels. A hydrogen bond donor/acceptor in this position may be a critical channel function because the T361C mutant channel was found to be functional (Wu et al., 2000). Closed-channel verapamil block of TIIA, TIIIA, and TIVA was measured in Ba^{2+} and Ca^{2+} at 0.05 Hz as described above (Fig. 9A). The TIIA, TIIIA, and TIVA mutants did not differ from WT channels in the fraction of current remaining in the presence of 30 μM verapamil when 10 mM Ba^{2+} was used as the charge carrier. In Ca^{2+}, TIIA, TIIIA, and TIVA were all less sensitive to verapamil block at 0.05 Hz than WT channel (i.e., Ca^{2+} potentiation of verapamil block was disrupted). In Ba^{2+}, only TIIIA among the TA mutants accumulated significantly less frequency-dependent verapamil block at the end of a 20-pulse, 1-Hz train of depolarizations (Fig. 9B). In Ca^{2+}, both TIIA and TIIIA significantly reduced the accumulation of verapamil block at 1 Hz (Fig. 9C). Thus, whereas TIIA, TIIIA, and TIVA all reduced the sensitivity of closed channels to verapamil in Ca^{2+}, only TIIA and TIIIA disrupted frequency-dependent block.

Inactivation and Ion Permeability in the Thr-to-Ala Mutants. Since the Thr-to-Ala mutations had the unexpected effect of disrupting Ca^{2+} potentiation of closed-channel verapamil block, we examined the effect of these mutations on Ca^{2+} acceleration of inactivation kinetics and ion permeability. Figure 10A shows normalized, averaged cur-

$V_{1/2})/k]\}$, where V is in the absence and presence of 30 μM verapamil were −15.9 ± 0.6 and −32.9 ± 0.4 mV, respectively. For WT channels, k values were −7.2 and −10.3 in the absence and presence of verapamil, respectively. For EIIIQ channels, k values were −10.8 and −8.4 in the absence and presence of verapamil, respectively. Time course of recovery from inactivation for WT (B) and EIIIQ (C) channels in the absence (closed symbols) and presence (open symbols) of 30 μM verapamil. Recovery from inactivation produced by a 1-s depolarization to +10 mV from a holding potential of −60 mV was measured using 50-ms test pulses to +10 mV after recovery intervals of 0.01, 0.1, 0.5, 1, 10, 20, and 30 s at −60 mV. The fraction of current recovered was plotted against the recovery interval. In both cases, the time course of recovery was fit to a double-exponential equation, representing fast and slow phases of recovery. For WT channels in the absence of verapamil, the time constants of recovery were τ_{fast} = 0.28 s and τ_{slow} = 6.88s, and the fraction of channels recovering with the fast time constant (f_{fast}) was 0.60. In the presence of 30 μM verapamil, τ_{fast} = 1.83 s, τ_{slow} = 41.0 s, and f_{fast} = 0.54. In the absence of verapamil, the time constants and the fraction of channels recovering for EIIIQ channels were τ_{fast} = 0.21 s, τ_{slow} = 16.9 s, and f_{fast} = 0.46. In the presence of 30 μM verapamil, the time constants for EIIIQ recovery were τ_{fast} = 1.91 s, τ_{slow} = 8.07 s, and f_{fast} = 0.61.

rent traces for WT and the Thr-to-Ala mutants in 10 mM Ba^{2+} or Ca^{2+}. We compared the extent of inactivation in these channels by measuring the percentage of peak current inactivated at the end of a 1-s depolarization to +10 mV from a holding potential of −60 mV (Fig. 10B). No significant difference in the extent of inactivation was observed among WT, TIIA, TIIIA, TIVA, and the domain III mutant F1117G in Ba^{2+}. In Ca^{2+}, only the TIIA mutant exhibited a decrease in the percentage of current inactivated at 1 s compared with WT. However, Ca^{2+} significantly increased the extent of inactivation at 1 s compared with Ba^{2+} in all three Thr-to-Ala mutants (i.e., Ca^{2+}- dependent inactivation was intact).

We also examined the permeability of the Thr-to-Ala mutants for Ba^{2+} relative to Ca^{2+}. Figure 11A shows whole-cell currents recorded in the same cell in the presence of 10 mM Ba^{2+} or Ca^{2+} in tsA 201 cells expressing WT and the indicated mutant $Ca_v1.2$ channels. Current was elicited by 100-ms depolarizations to +10 mV at 0.05 Hz, from a holding potential of −60 mV while the extracellular solution was switched between 10 mM Ba^{2+} and 10 mM Ca^{2+}. With Ca^{2+} as the charge carrier, the peak amplitude current measured in WT and TIVA channels was reduced relative to the peak current measured in Ba^{2+}. In contrast, the peak current amplitudes measured in Ca^{2+} were greater than those measured in Ba^{2+} for the TIIA and TIIIA mutants. Figure 11B shows the relative change in current amplitude, for each of the channels tested, upon switching from Ba^{2+}- to Ca^{2+}-containing extracellular solution. Thus, whereas the Thr-to-Ala mutations disrupt Ca^{2+} potentiation of verapamil block of closed channels, they do not eliminate Ca^{2+}-dependent inactivation. Furthermore, the TIIA and TIIIA mutations mediate an increased permeability of $Ca_v1.2$ for Ca^{2+} relative to Ba^{2+}.

Discussion

Distinct Effects of Selectivity Filter Mutants on Ca^{2+} Potentiation of Closed-Channel Block and Frequency-Dependent Block

We have shown that mutation of any of the selectivity filter glutamates does not reduce the sensitivity of $Ca_v1.2$ channels to closed-channel verapamil block in Ba^{2+} (Fig. 3). In a previous study, EIIIQ and EIVQ increased the IC_{50} of the nearly identical compound, desmethoxyverapamil (D888), by 15- and 20-fold, respectively, at a stimulation frequency of 0.1 Hz in 10 mM Ba^{2+}. D888 is more potent than verapamil in blocking $Ca_v1.2$ (Hockerman et al., 1995) and binding to $Ca_v1.1$ (Goll et al., 1984). A binding site between IIIS6 (Hockerman et al., 1997a) and IVS6 (Hockerman et al., 1995) was shown to account for the higher affinity of D888 for $Ca_v1.2$ at low-frequency stimulation. Furthermore, mutation of the three amino acids in IVS6 critical for high-affinity D888 block of $Ca_v1.2$ did not affect the potency of verapamil block at 0.1 Hz (Johnson et al., 1996). Thus, the present study supports previous work suggesting that D888 and verapamil interact with distinct binding determinants on closed $Ca_v1.2$ channels (i.e., at low-frequency stimulation).

I1627A is unique among the mutants used in this study because it is in the cytoplasmic C-terminal tail, not, apparently, in the vicinity of the transmembrane segments com-

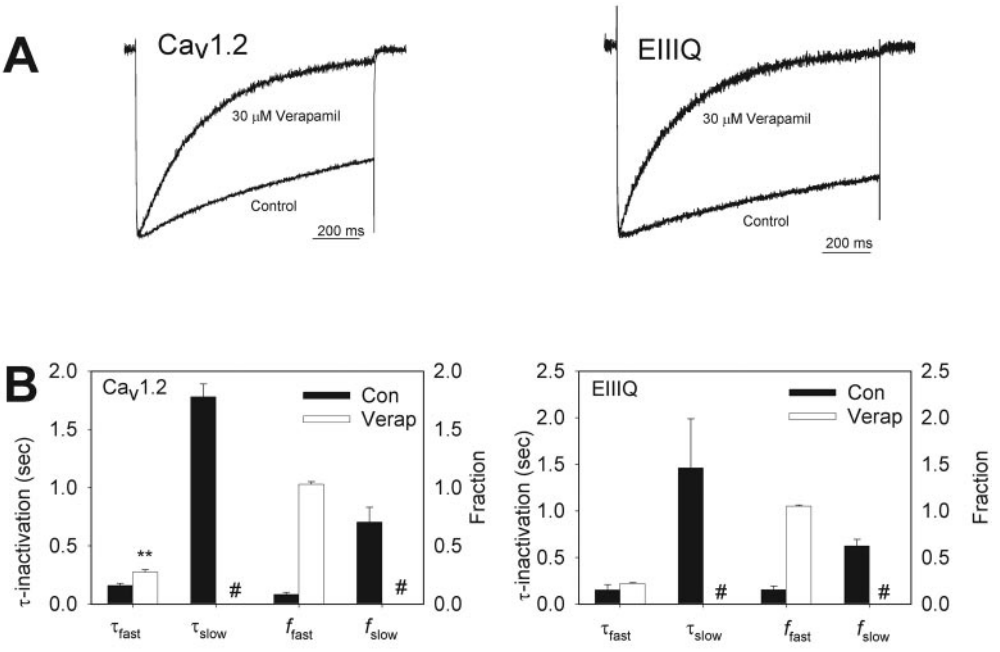

Fig. 7. Onset of verapamil block of depolarized WT and EIIIQ channels. A, representative traces of Ba^{2+} current through WT (left) and EIIIQ (right) channels measured during a 1-s depolarization to +10 mV, from a holding potential of −60 mV, in the absence (control) or presence of 30 μM verapamil. B, time course of inactivation in the absence (filled bars) and presence (open bars) of 30 μM verapamil for WT $Ca_v1.2$ (left) and EIIIQ (right). In the absence of verapamil, WT inactivation was fit by a double-exponential equation with a fast time constant (τ_F = 0.16 ± 0.02 s) and a slow time constant (τ_S = 1.78 ± 0.11 s) corresponding to the fraction fast (f_F = 0.10 ± 0.02) and the fraction slow (f_S = 0.70 ± 0.13). In the presence of 30 μM verapamil, WT inactivation was single-exponential with a relatively fast time constant (τ_F = 0.29 ± 0.02 s). In the absence of drug, EIIIQ channel inactivation was fit to a double-exponential equation with a fast time constant similar to that of WT channels (τ_F = 0.15 ± 0.06 s; f_F = 0.12 ± 0.04) and a slow time constant (τ_S = 1.46 ± 0.53 s; f_S = 0.62 ± 0.07). In the presence of 30 μM verapamil, EIIIQ channels displayed a single fast component of inactivation (τ_F = 0.21 ± 0.01 s). The asterisks indicate significant differences between the indicated parameter in the presence and absence of 30 μM verapamil (Student's t test; ⋆⋆, $P < 0.01$) (mean ± S.E., n = 3–6; #, not detected).

posing the small-molecule drug binding sites. However, as we previously observed with diltiazem (Dilmac et al., 2003), I1627A increased the sensitivity of closed $Ca_v1.2$ channels to verapamil block in Ba^{2+}, whereas frequency-dependent block was not different from WT in Ba^{2+} or Ca^{2+}. The I1627A mutation shifted the voltage dependence of inactivation by approximately −20 mV compared with WT. Because we found that closed-channel block of I1627A by 30 μM verapamil from a holding potential of −80 mV was not different from that of WT measured from a holding potential of −60 mV, it seems that the increase in sensitivity to verapamil in I1627A at −60 mV results from the shift in voltage dependence of inactivation. However, Ca^{2+} potentiation of closed-channel block of I1627A by verapamil is abolished at both potentials. These results suggest that Ca^{2+}-calmodulin binding to the C-terminal IQ motif, which is disrupted in I1627A (Zuhlke et al., 1999), may be required for Ca^{2+} potentiation of closed-channel verapamil block. The loss of Ca^{2+} potentiation of closed-channel block in all of the EQ mutations suggests that Ca^{2+} potentiation also requires Ca^{2+} binding in the channel pore. Taken together with our previous observation that Ca^{2+}-dependent inactivation is disrupted in the EQ mutations (Dilmac et al., 2003), these results also suggest that the consequences of Ca^{2+}-calmodulin binding to the C-terminal tail of $Ca_v1.2$ may include conformational changes in the pore region of the channel.

Ca^{2+} potentiation of closed-channel verapamil block was disrupted by mutation of any of the Glu-to-Gln mutants, F1117G, and all of the Thr-to-Ala mutants. The modulation of verapamil block by Ca^{2+} is distinct from what we previously observed for diltiazem (Dilmac et al., 2003), where EIIIQ, EIVQ, and F1117G, but not EIQ or EIIQ, disrupted Ca^{2+} potentiation of closed-channel diltiazem block. However, the effect of the Thr-to-Ala mutations on this property of diltiazem block was not examined in that study. Similar to diltiazem, DHPs bind in a pocket composed of IIIS5, IIIS6, and IVS6 (Hockerman et al., 1997c). Moreover, Ca^{2+} potentiation of DHP binding also requires Glu1118, Glu1419, and Phe1117 but not Glu363 or Glu709 (Peterson and Catterall, 1995). Taken together, these data suggest that Ca^{2+} binding to a site in domains III and IV modulates the diltiazem (Hockerman et al., 2000) and DHP (Hockerman et al., 1997c)

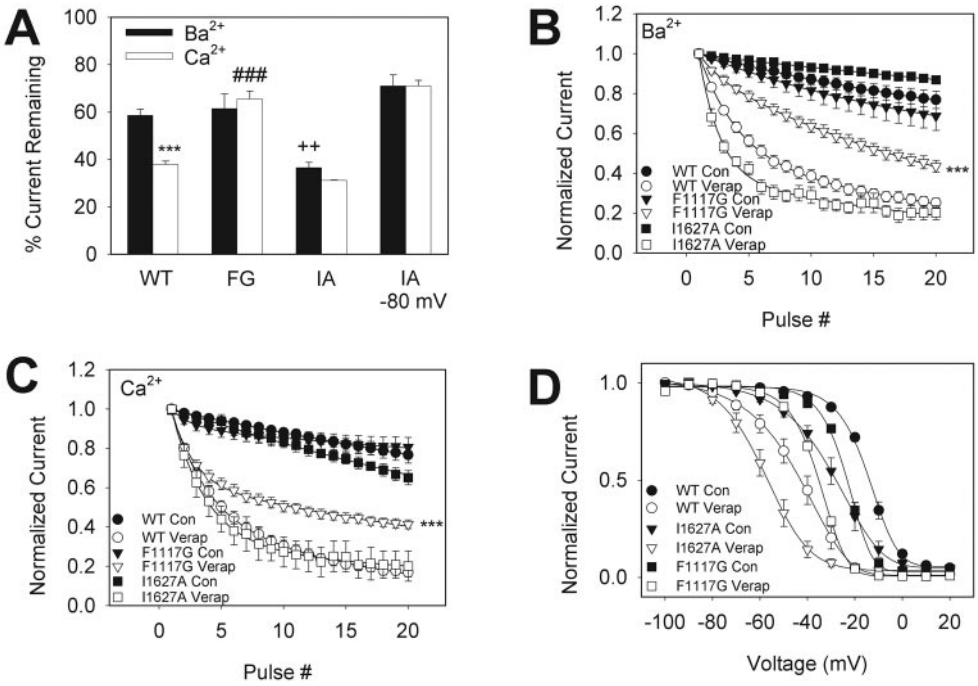

Fig. 8. Frequency and Ca^{2+} modulation of verapamil block in F1117G and I1627A. A, verapamil (30 μM) block of WT, F1117G, and I1627A $Ca_v1.2$ channels in 10 mM Ba^{2+} (closed bars) or 10 mM Ca^{2+} (open bars) at 0.05 Hz. The percentage of current remaining (mean ± S.E., n = 3–9) in each case was WT_{Ba} = 58.6 ± 2.6; WT_{Ca} = 37.8 ± 1.5; $F1117G_{Ba}$ = 61.4 ± 6.2; $F1117G_{Ca}$ = 65.5 ± 3.3.; $I1627A_{Ba}$ = 36.4 ± 2.4; and $I1627A_{Ca}$ = 31.0 ± 0.3. The percentage of current remaining for I1627A when measured from a holding potential of −80 mV was 70.1 ± 4.7 (n = 5) in 10 mM Ba^{2+}, and 71.0 ± 2.3 (n = 4) in 10 mM Ca^{2+}. Asterisks indicate a significant difference between current remaining in Ba^{2+} and Ca^{2+} (Student's t test; ★★★, $P <$ 0.001). The percentage of current remaining in Ba^{2+} for I1627A was significantly different from both WT and F1117G when measured from a holding potential of −60 mV (one-way ANOVA with Tukey's post hoc test; ++, $P < 0.01$). The percentage of current remaining for F1117G in Ca^{2+} was significantly different from both WT and I1627A (one-way ANOVA with Tukey's post hoc test; # # #, $P < 0.001$). B and C, frequency-dependent block of the indicated channels (mean ± S.E., n = 3–8) was measured as described in Figs. 4 and 5 in Ba^{2+} or Ca^{2+} in the absence (closed symbols) and presence (open symbols) of 30 μM verapamil. Smooth lines are fits of the data to a single-exponential equation, and these fits indicate that block reaches equilibrium at 25, 28, and 22% of control current in Ba^{2+}, and at 17, 43, and 21% of control current for WT, F1117G, and I1627A, respectively. In either Ba^{2+} or Ca^{2+}, only F1117G was significantly different from WT in the extent of block at the end of the 20-pulse, 1-Hz train of depolarizations (Student's t test; ★★★, $P < 0.001$). D, the voltage dependence of inactivation was measured as described in Fig. 6A. Measured Ba^{2+} currents were plotted against the conditioning pulse voltage in the absence (closed symbols) or presence (open symbols) of 30 μM verapamil. The data were fit to a Boltzman equation as in Fig. 6A. $V_{1/2}$ values for WT channels in the absence and presence of 30 μM verapamil were −13.7 ± 0.5 and −43.5 ± 0.8 mV, respectively. $V_{1/2}$ values for F1117G channels in the absence and presence of 30 μM verapamil were −23.4 ± 0.5 and −35.4 ± 0.3 mV, respectively. $V_{1/2}$ values for I1627A channels in the absence and presence of 30 μM verapamil were −28.4 ± 0.8 and −57.4 ± 0.9 mV, respectively. Slope (k) values for WT were −7.2 and −10.3 in the absence and presence of verapamil, respectively. Slope (k) values for F1117G were −5.8 and −6.0 in the absence and presence of verapamil, respectively. Slope (k) values for I1627A channels were −11.52 and −10.39 in the absence and presence of verapamil, respectively.

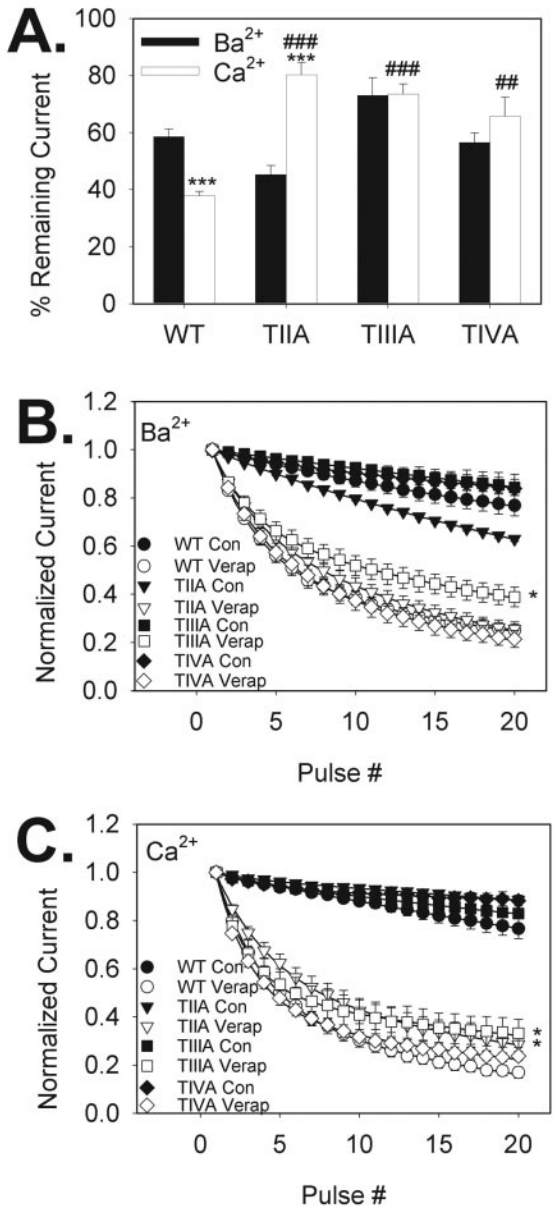

Fig. 9. Frequency and Ca^{2+} modulation of verapamil block of TIIA, TIIIA, and TIVA. A, Ca^{2+} potentiation of verapamil block at 0.05 Hz in 30 μM verapamil was measured as described in Fig. 5A, using either 10 mM Ba^{2+} (closed bars) or 10 mM Ca^{2+} (open bars) as the charge carrier. The percentage of current remaining in each case was (mean ± S.E.): WT_{Ba} = 58.6 ± 2.6; WT_{Ca} = 37.8 ± 1.5; $TIIA_{Ba}$ = 45.3 ± 3.2; $TIIA_{Ca}$ = 80.2 ± 4.2; $TIIIA_{Ba}$ = 73.0 ± 6.1; $TIIIA_{Ca}$ = 73.5 ± 3.6; $TIVA_{Ba}$ = 56.5 ± 3.4; and $TIVA_{Ca}$ = 65.7 ± 6.8. The percentage of current remaining in Ba^{2+} was not significantly different among WT and all of the mutants (one-way ANOVA). The percentage of current remaining in Ca^{2+} in each of the mutant channels was significantly different from that of WT (one-way ANOVA with Tukey's post hoc test; ##, $P < 0.01$; # # #, $P < 0.001$). The asterisks indicate significant differences between current remaining in Ba^{2+} and Ca^{2+} for WT and TIIA (Student's t test; ⋆⋆⋆, $P < 0.001$). B and C, frequency-dependent verapamil block of WT and the Thr-to-Ala mutant channels. Frequency-dependent verapamil block (percentage of current remaining; mean ± S.E, n = 3–8) of the indicated channels was measured as described in Figs. 4 and 5 in Ba^{2+} or Ca^{2+} in the absence (closed symbols) and presence (open symbols) of 30 μM verapamil. Smooth lines are fits of the data to a single-exponential equation, and these fits indicate that block reaches equilibrium at 25, 39, 22, and 19% of control Ba^{2+} current and 17, 35, 27, and 25% of control Ca^{2+} current for WT, TIIIA, TIIA, and TIVA, respectively. The TIIIA mutant was blocked to a significantly lesser extent than WT channels in both Ba^{2+} and Ca^{2+}, whereas the TIIA mutant was blocked to a significantly lesser extent than WT in Ca^{2+} (Student's t test; ⋆, $P < 0.05$).

binding sites, which include IIIS6 and IVS6, whereas Ca^{2+} binding to multiple sites in the selectivity filter is required for high-affinity verapamil block of closed channels. This scenario is consistent with a binding site for verapamil on closed channels that is distinct from that for DHPs and diltiazem.

Frequency Dependence of Verapamil Block in Ba^{2+} or Ca^{2+}. In contrast to our results using low-frequency stimulation (0.05 Hz), we found that multiple mutations clustered in the domain III region of the selectivity filter markedly disrupted frequency-dependent verapamil block (Figs. 4, 5, 8, and 9). Disruption of block was similar whether Ba^{2+} or Ca^{2+} was used as the charge carrier. Surprisingly, we found that, unlike our previous observations with diltiazem (Dilmac et al., 2003), frequency-dependent block of $Ca_v1.2$ is not appreciably potentiated by Ca^{2+} in our experimental system. In addition, the F1117G and EIIIQ mutations both significantly decreased the leftward shift in $V_{1/2}$ induced by 30 μM verapamil [F1117G, Δ = ~12 mV (Fig. 8D); EIIIQ, Δ = ~17 mV (Fig. 6A)] compared with that observed in WT $Ca_v1.2$ [Δ = ~30 mV (Fig. 6A)]. Furthermore, the EIIIQ mutation increases the rate of recovery from depolarized-channel verapamil block compared with WT $Ca_v1.2$ (Fig. 6, B and C) but

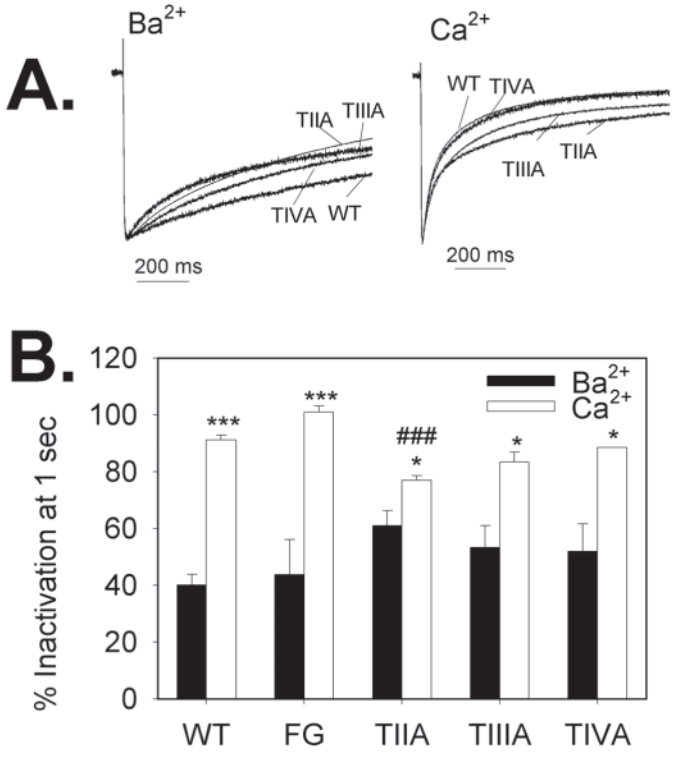

Fig. 10. Inactivation properties of WT and the mutant channels TIIA, TIIIA, and TIVA in Ba^{2+} and Ca^{2+}. A, averaged, normalized current traces for WT channels and each of the indicated mutant channels elicited during a 1-s depolarization to +10 mV from a holding potential of −60 mV in extracellular solution containing 10 mM Ba^{2+} (left) or 10 mM Ca^{2+} (right) are shown. B, summary of the percentage of channels inactivated at the end of a 1-s depolarization in Ba^{2+} or Ca^{2+}. All channels tested displayed significant increases in the percentage of channels inactivated at the end of a 1-s depolarization in Ca^{2+} compared with Ba^{2+} (mean ± S.E, n = 3–7; Student's t test; ⋆, $P < 0.05$; ⋆⋆⋆, $P < 0.001$). There was no significant difference in the percentage of inactivated channels in Ba^{2+} among WT and mutant channels (one-way ANOVA). In Ca^{2+}, the percentage of channels inactivated at 1 s was significantly less in TIIA than in WT channels (WT_{Ca} = 91.1 ± 1.7%, n = 7; $TIIA_{Ca}$ = 77.0 ± 1.6%, n = 5; # # #, $P < 0.001$; one-way ANOVA with Tukey's post hoc test).

does not affect the shift of channels to the fast-inactivating state induced by verapamil (Fig. 7B). Our finding that verapamil accelerates the inactivation of $Ca_v1.2$ channels and increases the fraction of channels inactivating is consistent with previous studies (Johnson et al., 1996; Sokolov et al., 2001). However, our results with EIIIQ are in contrast to observations with mutations in IVS6 which accelerated both verapamil block and recovery from verapamil block at +10 mV (Johnson et al., 1996). The effect of the F1117G mutation on frequency-dependent verapamil block seems to be Ca^{2+}-dependent, because a fit of the data to a single exponential function indicates that steady-state block of F1117G in Ba^{2+} is not different from that of WT $Ca_v1.2$, although the current remaining at the 20th pulse is clearly different from that of WT (Fig. 8B). We examined the inactivation rate of F1117G in the presence and absence of 30 μM verapamil in Ba^{2+} and did not find any significant difference from WT (N. Dilmac and G. H. Hockerman, unpublished data). It is not clear how the F1117G mutant is specifically slowing development of frequency-dependent verapamil block in Ba^{2+}. However, it is clear that F1117G decreases affinity for verapamil in Ca^{2+}, because both the steady-state block determined from a fit of the data and the current remaining at the 20th pulse are clearly different from that of WT (Fig. 8C). Likewise, TIIA disrupts both closed-channel and frequency-dependent verapamil in Ca^{2+} but not in Ba^{2+} (Fig. 9). Our data support a scenario in which frequency-dependent verapamil block of $Ca_v1.2$ channels (i.e., channels in the open and/or inactivated state) involves binding to a site that includes Thr1116, F1117G, Glu1118, and Glu1419, which may be accessed from the intracellular mouth of the pore. Taken together, our results suggest that verapamil may block closed channels and open/inactivated channels by binding to distinct sites, which include TIIA as a common determinant in Ca^{2+}. This scenario was proposed previously based upon experiments using a membrane-impermeable, quaternary ammonium derivative of D888. These experiments suggested that closed-channel block was mediated by a binding site accessible from the extracellular surface of the channel, whereas frequency-dependent block was mediated by a binding site accessible from the intracellular side of the membrane (Berjukov et al., 1996). In addition, our finding that, with the exception of Phe1117, the molecular determinants for frequency-dependent verapamil block are conserved among voltage-gated Ca^{2+} channels (i.e., Thr1116, Glu1118, Glu1419) may explain the relatively low discrimination of L-type and non-L-type Ca^{2+} channels by verapamil (Diochot et al., 1995; Ishibashi et al., 1995).

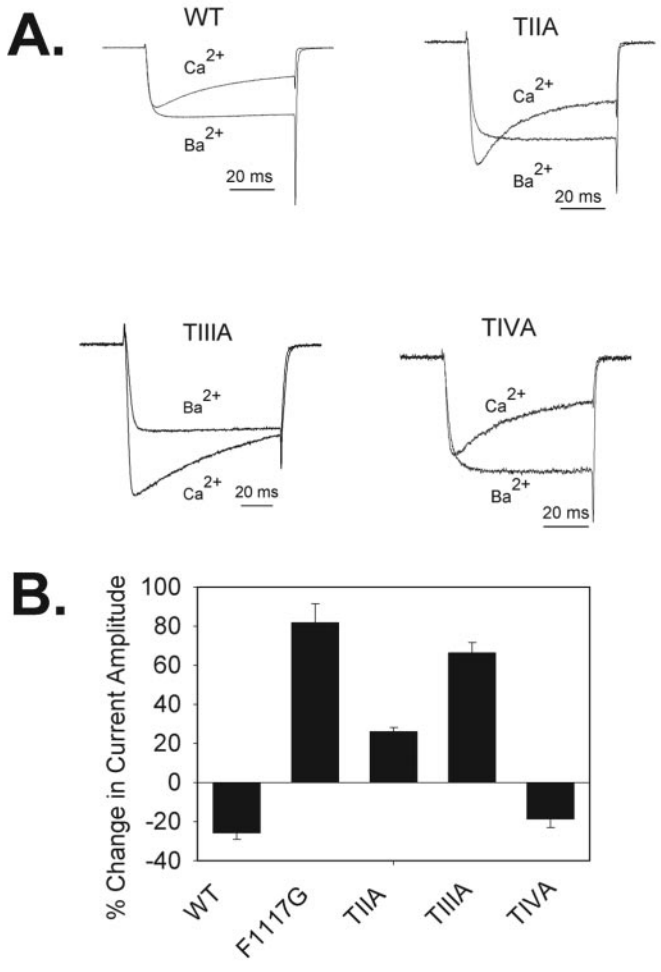

Fig. 11. Permeability of Ca^{2+} relative to Ba^{2+} in WT and mutant $Ca_v1.2$ channels. A, current traces recorded from single tsA 201 cells expressing WT, TIIA, TIIIA, and TIVA mutant channels recorded in 10 mM Ba^{2+} or 10 mM Ca^{2+}. Current was elicited using a 100-ms depolarization to +10 mV from a holding potential of −60 mV. Note the increase in peak current in Ca^{2+} relative to peak current in Ba^{2+} in the TIIA and TIIIA mutants. B, change in peak current amplitude measured at +10 mV from a holding potential of −60 mV when the extracellular solution is switched from 10 mM Ba^{2+} to 10 mM Ca^{2+}. The values shown are mean ± S.E. (n = 3–10) for WT $Ca_v1.2$ channels and each of the indicated mutants.

Conserved Residues Thr707, Thr1116, and Thr1417 and $Ca_v1.2$ Activity in Ca^{2+}. Our observation that the conserved Thr residues adjacent to the selectivity filter glutamates contribute to Ca^{2+} modulation of verapamil block of closed channels was unexpected. We had previously shown that the EIIQ, EIIIQ, and EIVQ mutations disrupt Ca^{2+}-dependent inactivation, and EIIIQ and EIVQ increase the permeability of Ca^{2+} relative to Ba^{2+} (Dilmac et al., 2003). Therefore, we examined these properties of channel activity in the Thr-to-Ala mutants. Our finding that none of the Thr-to-Ala mutations disrupts Ca^{2+}-dependent inactivation (Fig. 10) is consistent with our observations with the F1117G mutant, which disrupts Ca^{2+} modulation of diltiazem and verapamil block but does not disrupt Ca^{2+}-dependent inactivation. Our observations with the Thr-to-Ala mutants also further highlight the specific role of the selectivity filter Glu residues, among other adjacent residues, in mediating Ca^{2+}-dependent inactivation. However, Thr707 and Thr1116, as well as Phe1117, apparently play a role in forming the ion permeation pathway, because mutation of these residues increases the permeability of Ca^{2+} relative to Ba^{2+} (Fig. 11).

In summary, we have shown that Ca^{2+} potentiation of closed-channel block of $Ca_v1.2$ by verapamil requires all four selectivity filter glutamates, whereas amino acid residues adjacent to the selectivity filter in domain III contribute to the high-affinity binding of verapamil to the depolarized state of the channel. Furthermore, because Ca^{2+} does not potentiate frequency-dependent verapamil block, Ca^{2+} is not likely to potentiate binding of verapamil to the depolarized state of the channel. Our results further differentiate the molecular mechanisms of verapamil and diltiazem block of $Ca_v1.2$, suggest that distinct binding sites may mediate verapamil block of closed and depolarized channels, and sug-

gest that common molecular determinants may mediate the block of non-L-type voltage-gated Ca^{2+} channels by verapamil.

References

Almers W and McCleskey EW (1984) Non-selective conductance in calcium channels of frog muscle: calcium selectivity in a single-file pore. *J Physiol* **353:**585–608.

Berjukov S, Aczel S, Beyer B, Kimball SD, Dichtl M, Hering S, and Striessnig J (1996) Extra- and intracellular action of quaternary devapamil on muscle L-type Ca^{2+}-channels. *Br J Pharmacol* **119:**1197–1202**.**

Bers DM and Perez-Reyes E (1999) Ca channels in cardiac myocytes: structure and function in Ca influx and intracellular Ca release. *Cardiovasc Res* **42:**339–360.

Cai D, Mulle JG, and Yue DT (1997) Inhibition of recombinant Ca^{2+} channels by benzothiazepines and phenylalkylamines: class-specific pharmacology and underlying molecular determinants. *Mol Pharmacol* **51:**872–881.

Dilmac N, Hilliard N, and Hockerman GH (2003) Molecular determinants of Ca^{2+} potentiation of diltiazem block and Ca^{2+}-dependent inactivation in the pore region of $Ca_v1.2$. *Mol Pharmacol* **64:**491–501.

Diochot S, Richard S, Baldy-Moulinier M, Nargeot J, and Valmier J (1995) Dihydropyridines, phenylalkylamines, and benzothiazepines block N-, P/Q- and R-type calcium currents. *Pflueg Arch Eur J Physiol* **431:**10–19.

Doring F, Degtiar VE, Grabner M, Striessnig J, Hering S, and Glossman H (1996) Transfer of L-type calcium channel IVS6 segment increases phenylalkylamine sensitivity of α1a. *J Biol Chem* **271:**11745–11749.

Ellis SB, Williams ME, Ways NR, Brenner R, Sharp AH, Leung AT, Campbell KP, McKenna E, Koch WJ, Hui A, et al. (1988) Sequence and expression of mRNAs encoding the alpha 1 and alpha 2 subunits of a DHP-sensitive calcium channel. *Science (Wash DC)* **241:**1661–1664.

Fleckenstein A and Fleckenstein-Grun G (1980) Cardiovascular protection by Ca antagonists. *Eur Heart J* **1 (Suppl B):**15–21.

Goll A, Ferry DR, Striessnig J, Schober M, and Glossmann H (1984) (−)-[^{3}H]Desmethoxyverapamil, a novel Ca^{2+} channel probe. Binding characteristics and target size analysis of its receptor in skeletal muscle. *FEBS Lett* **176:**371–377.

Hockerman GH, Dilmac N, Scheuer T, and Catterall WA (2000) Molecular determinants of diltiazem block in domains IIIS6 and IVS6 of L-type Ca^{2+} channels. *Mol Pharmacol* **58:**1264–1270.

Hockerman GH, Johnson BD, Abbott MR, Scheuer T, and Catterall WA (1997a) Molecular determinants of high affinity phenylalkylamine block of L-type calcium channels in transmembrane segment IIIS6 and the pore region of the α1 subunit. *J Biol Chem* **272:**18759–18765.

Hockerman GH, Johnson BD, Scheuer T, and Catterall WA (1995) Molecular determinants of high affinity phenylalkylamine block of L-type calcium channels. *J Biol Chem* **270:**22119–22122.

Hockerman GH, Peterson BZ, Johnson BD, and Catterall WA (1997b) Molecular determinants of drug binding and action on L-type calcium channels. *Annu Rev Pharmacol Toxicol* **37:**361–396.

Hockerman GH, Peterson BZ, Sharp E, Tanada TN, Scheuer T, and Catterall WA (1997c) Construction of a high-affinity receptor site for dihydropyridine agonists and antagonists by single amino acid substitutions in a non-L-type Ca^{2+} channel. *Proc Natl Acad Sci USA* **94:**14906–14911.

Ishibashi H, Yatani A, and Akaike N (1995) Block of P-type Ca^{2+} channels in freshly dissociated rat cerebellar Purkinje neurons by diltiazem and verapamil. *Brain Res* **695:**88–91.

Johnson BD, Hockerman GH, Scheuer T, and Catterall WA (1996) Distinct effects of mutations in transmembrane segment IVS6 on block of L-type calcium channels by structurally similar phenylalkylamines. *Mol Pharmacol* **50:**1388–1400.

Jones SW (1998) Overview of voltage-dependent calcium channels. *J Bioenerg Biomembr* **30:**299–312.

Lee KS and Tsien RW (1983) Mechanism of calcium channel blockade by verapamil, D600, diltiazem and nitrendipine in single dialysed heart cells. *Nature (Lond)* **302:**790–794.

Nawrath H and Wegener JW (1997) Kinetics and state-dependent effects of verapamil on cardiac L-type calcium channels. *Naunyn Schmiedeberg's Arch Pharmacol* **355:**79–86.

Peterson BZ and Catterall WA (1995) Calcium binding in the pore of L-type calcium channels modulates high affinity dihydropyridine binding. *J Biol Chem* **270:** 18201–18204.

Peterson BZ, DeMaria CD, Adelman JP, and Yue DT (1999) Calmodulin is the Ca^{2+} sensor for Ca^{2+}-dependent inactivation of L-type calcium channels. *Neuron* **22:** 549–558.

Pragnell M, Sakamoto J, Jay SD, and Campbell KP (1991) Cloning and tissue-specific expression of the brain calcium channel beta-subunit. *FEBS Lett* **291:**253–258.

Snutch TP, Tomlinson WJ, Leonard JP, and Gilbert MM (1991) Distinct calcium channels are generated by alternative splicing and are differentially expressed in the mammalian CNS. *Neuron* **7:**45–57.

Sokolov S, Timin E, and Hering S (2001) On the role of Ca^{2+}- and voltage-dependent inactivation in Ca(v)1.2 sensitivity for the phenylalkylamine (−)gallopamil. *Circ Res* **89:**700–708.

Tanabe T, Takeshima H, Mikami A, Flockerzi V, Takahashi H, Kangawa K, Kojima M, Matsuo H, Hirose T, and Numa S (1987) Primary structure of the receptor for calcium channel blockers from skeletal muscle. *Nature (Lond)* **328:**313–318.

Wu XS, Edwards HD, and Sather WA (2000) Side chain orientation in the selectivity filter of a voltage-gated Ca^{2+} channel. *J Biol Chem* **275:**31778–31785.

Yang J, Ellinor PT, Sather WA, Zhang JF, and Tsien RW (1993) Molecular determinants of Ca^{2+} selectivity and ion permeation in L-type Ca^{2+} channels. *Nature (Lond)* **366:**158–161.

Zuhlke RD, Pitt GS, Deisseroth K, Tsien RW, and Reuter H (1999) Calmodulin supports both inactivation and facilitation of L-type calcium channels. *Nature (Lond)* **399:**159–162.

Address correspondence to: Gregory Hockerman, 575 Stadium Mall Dr., West Lafayette, IN 47907-2091. E-mail: gregh@pharmacy.purdue.edu